Measurement of neutron activation cross sections

by p-Be semi-monoenergetic neutrons

T. Nakamura, H. Sugita, Y. Kondo, Y. Uwamino[*] and M. Imamura[*]

Cyclotron and Radioisotope Center, Tohoku University

[*]Institute for Nuclear Study, University of Tokyo

ABSTRACT

Neutron activation cross sections of C, Na, Mg, Al, Si, Ca, V, Cr, Mn, Cu, Zn and Au, which are mostly constituents of accelerator and building materials, in the energy range of 10 to 40 MeV, by using semi-monoenergetic neutrons from the Be(p,n) reaction. A proton beam of energies of 20, 22.5, 25, 27.5, 30, 32.5, 35, 37.5 and 40 MeV hits the 1-mm and 2-mm thick Be targets which are backed by the water coolant. The induced gamma-ray activities of the irradiated samples were measured with a pure Ge detector and of long-lived ^{26}Al were done by accelerator mass spectrometry. The activation cross section data could be obtained by unfolding technique.

I. INTRODUCTION

The radioactivities induced in accelerator and building materials, air and drain water by high energy particles, especially intense neutrons, cause severe external exposure to the workers in high energy intense accelerator facilities. To evaluate the induced radioactivities, the activation cross section data are of basic importance. The activation cross section data for protons have ever been published by several workers and for neutrons in the energy range of thermal to 20 MeV the evaluated data files exist such as ENDF/B-V and JENDL-3. While, on the other hand, there have been very few experimental data for neutrons of energy above 20 MeV and no evaluated data files.

Using a simple target system consisting of a Be disk backed by a water coolant, an intense semi-monoenergetic neutron field for activation experiment of energy up to 40 MeV was developed(1) at the SF cyclotron of the Institute for Nuclear Study, University of Tokyo. Activation experiment at this neutron field has been performed with natural samples of C, Na, Mg, Al, Si, Ca, V, Cr, Mn, Cu, Zn and Au.

II. NEUTRON FIELD FOR ACTIVATION EXPERIMENT

A proton beam of energies of 20, 22.5, 25, 27.5, 30, 32.5, 35, 37.5, 40 MeV is extracted from the SF cyclotron at the Institute for Nuclear Study, Univ. of Tokyo and hits the 1-mm thick (E_p = 20 to 37.5 MeV) and 2-mm thick (E_p = 40 MeV) Be targets which are backed by the water coolant. The water is simultaneously used to absorb the residual proton energy because of the small neutron production cross section of $^{16}O(p,n)$.

The neutron spectra at 0 deg were measured with a 51 mm diameter by 51 mm long NE-213 placed at 1.3 m from the Be target (1). An n-γ discrimination technique was utilized and the pulse height distribution by neutrons was unfolded to an energy spectrum with the revised FERDO code (2). The measured neutron spectra which subtracted the room-scattered components are shown with the unfolded errors in Fig. 1. In the figure, the monoenergetic peak neutron energy is indicated for each proton energy and the former is 4 to 5 MeV lower than the latter. The spectra also have low energy tails coming from the Be target and the water beam stopper.

III. MEASUREMENT OF INDUCED RADIOACTIVITY

The samples were irradiated by this semi-monoenergetic neutrons in the forward direction at 5 to 20 cm distant from the Be target. The proton beam current was kept to be several μA during the irradiation. The induced gamma-ray activities of the irradiated samples were measured with a pure Ge detector and the activation rates were obtained after the correction of self-absorption, parent-daughter decay and sum-coincidence effects. The measurement of long-lived ^{26}Al (half-life of 7.2 x 10^5 y) produced by $^{27}Al(n,2n)$ reaction was done by accelerator mass spectrometry(AMS) which has been equipped at the tandem Van-de-Graaf accelerator of the Research Center for Nuclear Science and Technology, Univ. of Tokyo (3). The $^{26}Al/^{27}Al$ isotopic ratios were obtained by AMS and were converted to the ^{26}Al activities.

IV. EVALUATION OF ACTIVATION CROSS SECTION

The measured activation rate, A_i is related to

$$A_i = N \int_0^{E_P} \sigma(E) \, \phi_i(E) \, dE,$$

where i : ith experiment corresponding to each proton energy, E_p

    N : number of target nucleus in a sample

  $\sigma(E)$: activation cross section

  $\phi_i(E)$: neutron spectrum shown in Fig. 1.

Since the neutron spectrum $\phi_i(E)$ is not purely monoenergetic but has low energy component, the $\sigma(E)$ value can be obtained by unfolding this integral equation. We finally obtained it with the SAND-II code of iterative perturbation method (4), the NEUPAC code using J-1 type unfolding method (5) and the least-square fitting (LSF) method. In the LSF, the absolute value of an initial guess of cross section was adjusted to the measured activation rates under the condition of preserving its shape as follows,

$$R = \Sigma \, (A_i - \int_0^{E_P} k \, N \, \sigma(E) \, \phi_i(E) \, dE)^2$$

where k is determined to make R minimum. These codes required the initial guess value of $\sigma(E)$ for unfolding, and they were calculated with the ALICE code (6), in case of the lack of any experimental and calculated data. The SAND-II code does not give unfolded errors, while on the other hand, the NEUPAC code gives the errors propagated from errors of initial guess values, neutron spectrum and activation rates.

V. RESULTS AND DISCUSSIONS

Most results of activation cross sections are the first experimental data that have been obtained above 20 MeV. Some results are exemplified in Figs. 2 to 6. Figure 2 shows the $^{27}Al(n,\alpha)^{24}Na$ cross section data. Our results unfolded by three codes, SAND-II, NEUPAC and LSF, agree quite well each other, except that a small bump around 25 MeV can only be seen by the SAND-II unfolding. Our data also show good agreement with the data by ENDF/B-V and Greenwood (7) as a whole, but are 5% smaller at a peak value around 13 MeV than them. The $^{23}Na(n,2n)^{22}Na$ cross sections are shown in Fig. 3. The experimental data and the theoretically evaluated data are largely dispersed and our results are

close to the experimental data by Maslov et al. and Menlove et al. (8), and to the IRDF-85 data file.

Figure 4 shows the $^{27}Al(n,2n)^{26}Al$ cross section data. Our results given by SAND-II and NEUPAC show very good agreement each other. Our experimental results give a little lower values than Iwasakis' newest experimental data around 15 MeV (9). For comparison, the experimental data of $^{27}Al(n,2n)^{26}Al^m$ (half-life of 6.3 sec) cross section by Mani et al. (10) are also shown in Fig. 4. The peak value of 150 mb at 20 MeV for $^{27}Al(n,2n)^{26}Al^m$ is 1.6 times larger than that of 95 mb at 20-24 MeV for $^{27}Al(n,2n)^{26}Al^g$, but the former value in the lower energy region is much smaller than the latter value.

For $^{nat}Si(n,XnYp)^{28}Al$ cross section data shown in Fig. 5, the SAND-II results have slightly larger peak value around 12 MeV than the NEUPAC results. Our results are compared with the theoretical $^{28}Si(n,p)^{28}Al$ cross section data given by the IAEA compilation (11), and are about 10 to 25 % smaller than the latter between 10 and 15 MeV. The $^{nat}Cu(n,Xn)^{62}Cu$ cross section data are shown in Fig. 6. Our results unfolded by three codes also show good agreement within their unfolded errors. The IAEA data for $^{63}Cu(n,2n)^{62}Cu$ (11) give about 30 to 40 % higher values than our results and the GNASH calculation for $^{nat}Cu(n,Xn)^{62}Cn$ by Yamamuro (12) gives closer values to our experimental data. The authors wish to thank to Drs. H. Nagai and K. Kobayashi and Mr. H. Yamashita for their kindful cooperation on the ^{26}Al measurement by the AMS system. This work was financially supported by a Grant-in-Aid for Cooperative Research of the Japanese Ministry of Culture and Education.

References

1 Y. Uwamino, T. Ohkubo, A. Torii and T. Nakamura, Nucl. Instr. Methods, A271, 546 (1988).

2 K. Shin, Y. Uwamino and T. Hyodo, Nucl. Technol., 53, 78 (1981).

3 H. Nagai, T. Kobayashi, M. Honda, M. Imamura, K. Kobayashi, K. Yoshida and H. Yamashita, Nucl. Instr. Methods, B29, 266 (1987).

4 W. N. McElroy, S. Berg, T. Crockett and R. G. Hawkins, AFWL-TR-67-41, Vols. I-IV, Air Force Weapons Laboratory (1967).

5 A. Sekiguchi, M. Nakazawa and N. Ueda, PNC J260 85-01, Power Reactor and Nuclear Fuel Development Corporation (1985).

6   M. Blann and J. Bisplingshoff, LLNL Report No. UCID 19614, Lawrence Livermore National Laboratory (1983).

7   L. R. Greenwood, ANL/FPP/TM-115, Argonne National Laboratory (1978).

8   Cited from D. C. Larson, Nucl. Sci. Eng., 78, 324 (1981).

9   S. Iwasaki, J. R. Dumais and K. Sugiyama, Proc. Intern. Conf. Nucl. Data for Sci. and Technol., Mito, ed. by S. Igarashi, (1988) 295.

10 G. S. Mani, G. J. McCallum and A. T. G. Ferguson, Nucl Phys., 19, 535 (1960).

11 International Atomic Energy Agency, "Handbook on Nuclear Activation Data", Technical Report Series No. 273 (1987).

12 N. Yamamuro, Private Communications (1990).
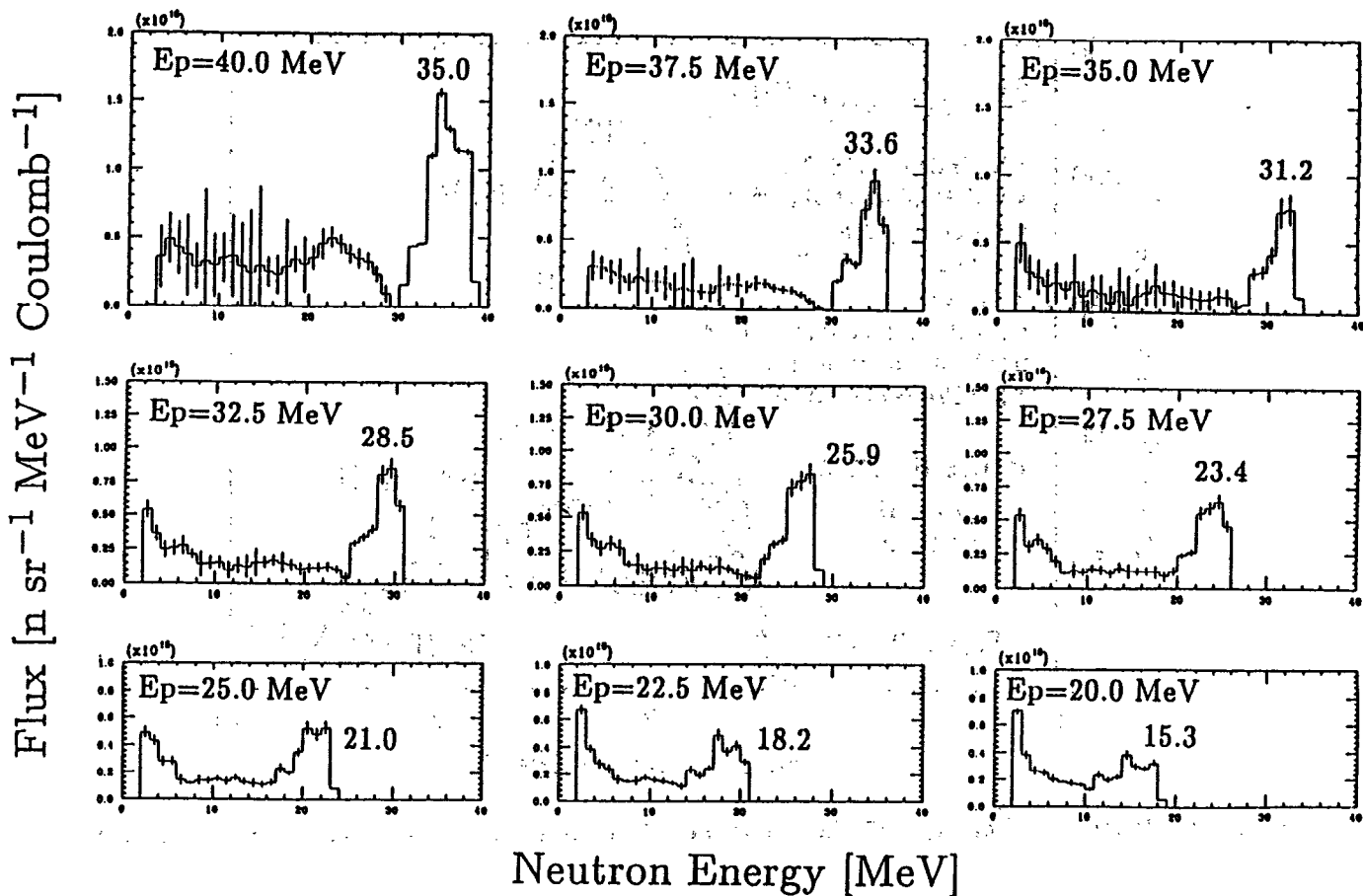
Fig. 1 Semi-monoenergetic neutron energy spectra for proton energies of 20, 22.5, 25, 27.5, 30, 32.5, 35, 37.5, 40 MeV
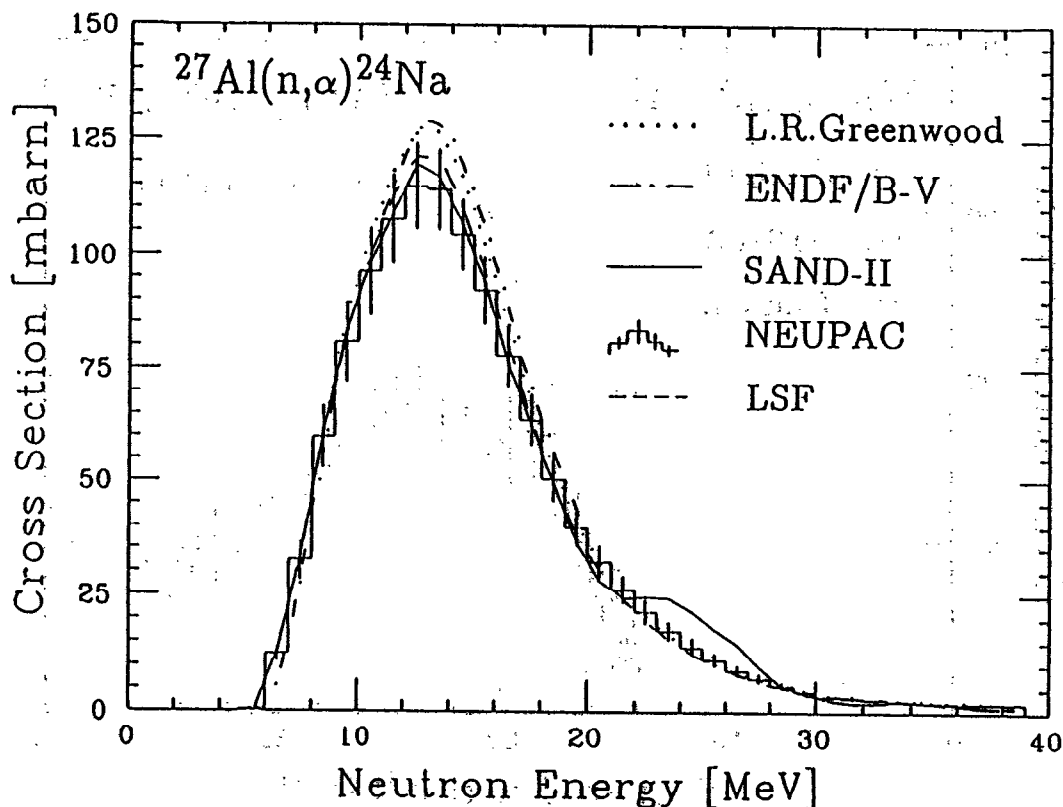

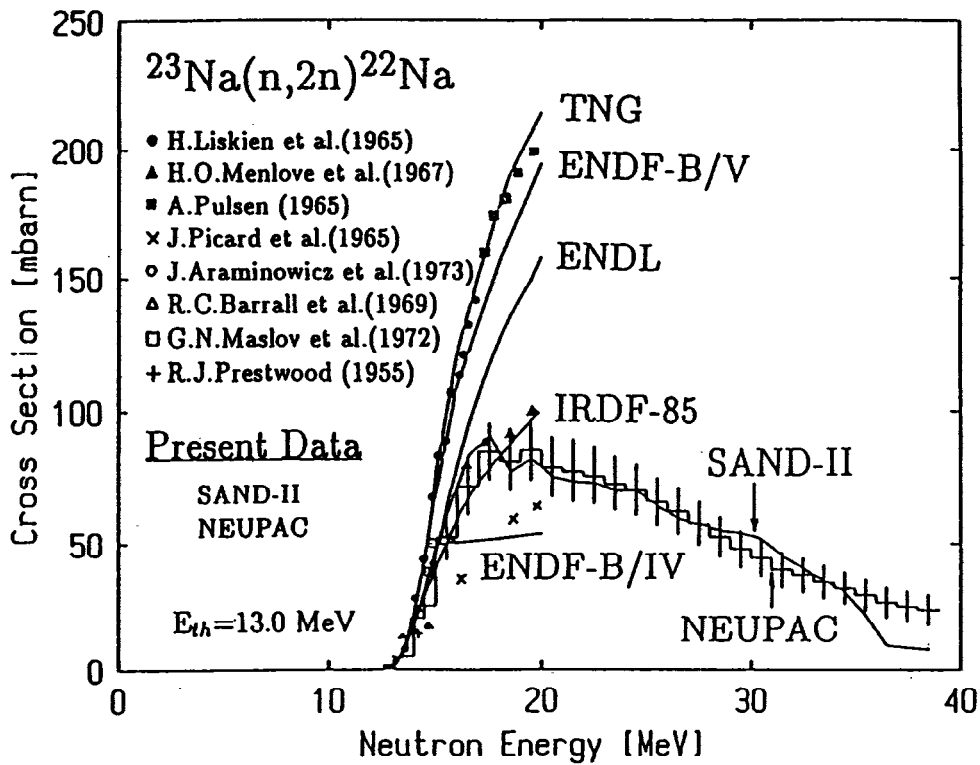Fig. 2 Measured ^{27}Al(n,α)^{24}Na cross section data, together with the cited data

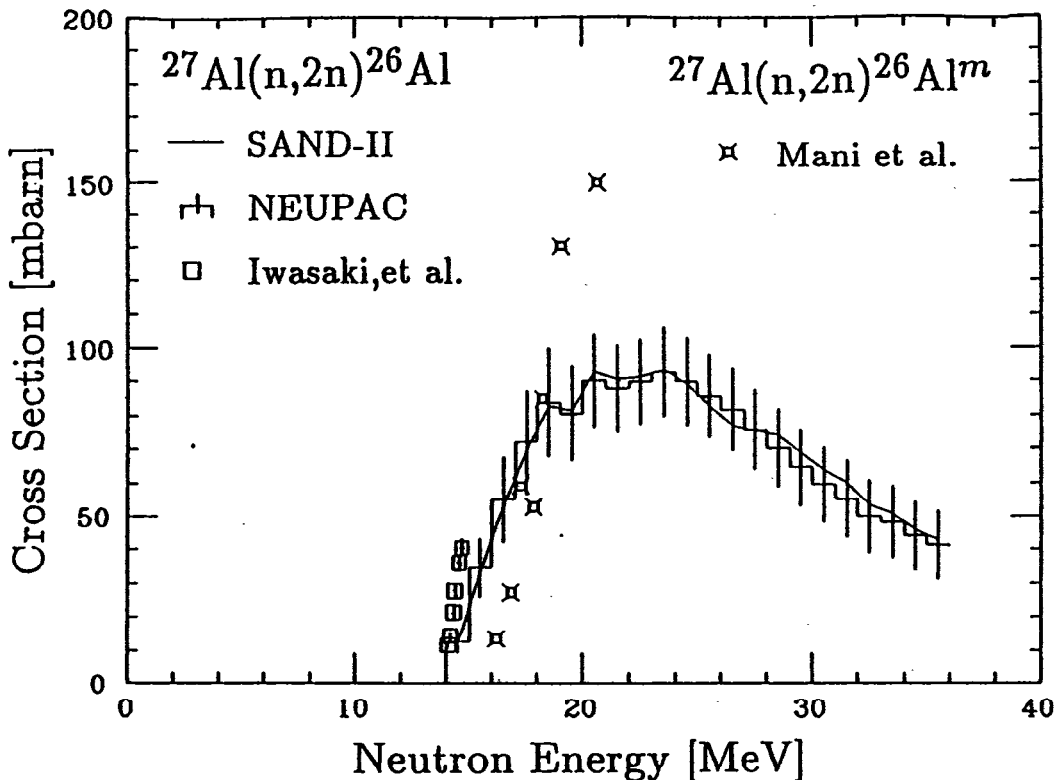Fig. 3 Measured ^{23}Na(n,2n)^{22}Na cross section data, together with the cited data

Fig. 4 Measured ^{27}Al(n,2n)^{26}Al cross section data, together with the cited data

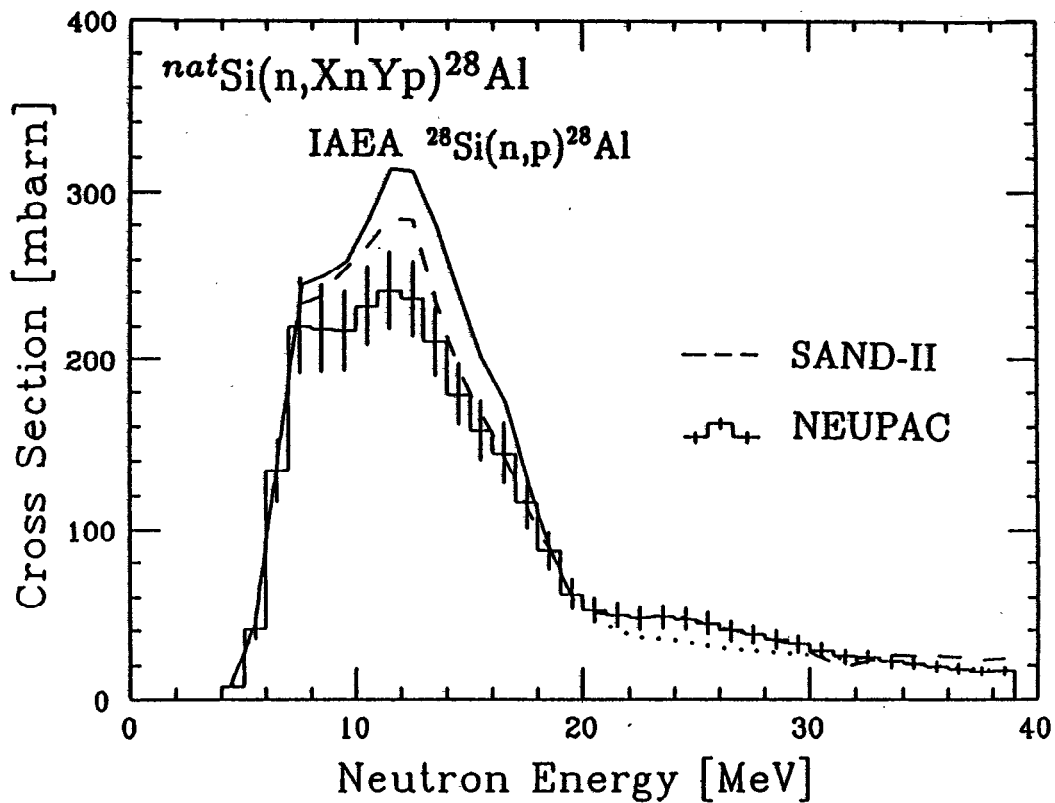Fig. 5 Measured $^{nat}Si(n,XnYp)^{28}Al$ cross section data, together with the cited data

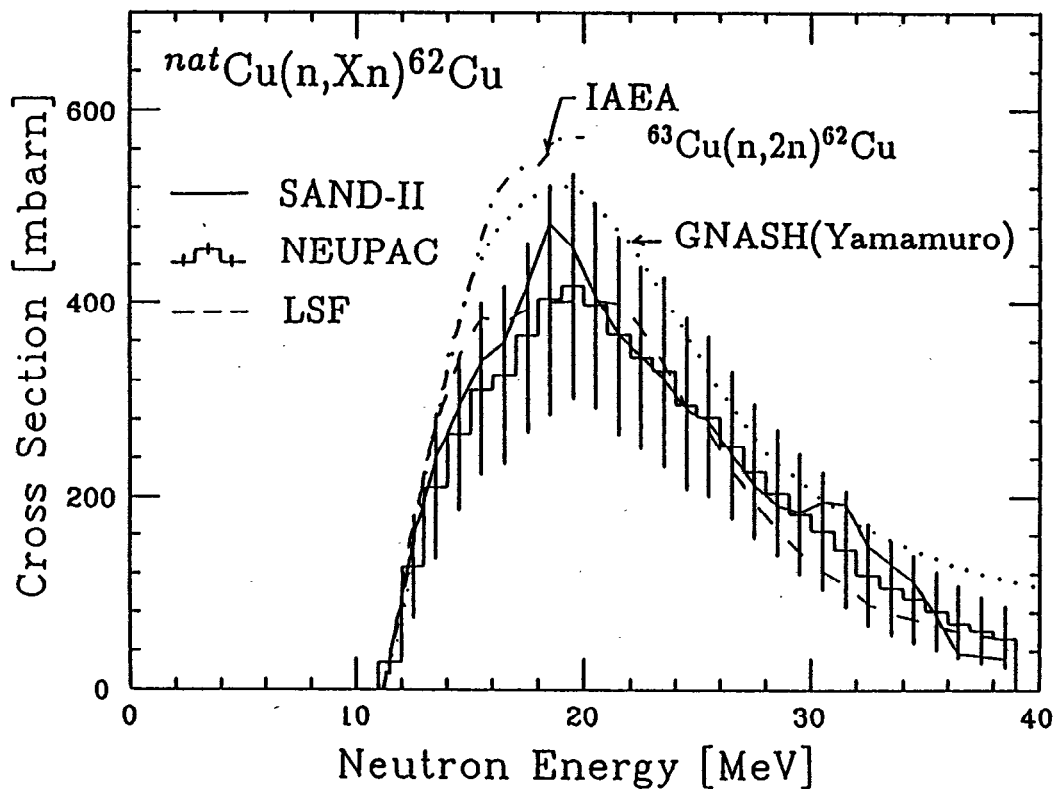Fig. 6 Measured $^{nat}Cu(n,Xn)^{62}Cu$ cross section data, together with the cited data